Title	Lysosomal membrane permeabilization is involved in oxidative stress-induced apoptotic cell death in LAMP2-deficient iPSCs-derived cerebral cortical neurons
Author(s)	LAW, CY; Siu, DCW; Fan, K; Lai, KWH; Au, KW; Lau, VYM; Wong, LY; Ho, JCY; Lee, YK; Tse, HF; Ng, KM
Citation	Biochemistry and Biophysics Reports, 2016, v. 5, p. 335-345
Issued Date	2016
URL	http://hdl.handle.net/10722/232015
Rights	Posting accepted manuscript (postprint): © <year>. This manuscript version is made available under the CC-BY-NC-ND 4.0 license http://creativecommons.org/licenses/by-nc-nd/4.0/; This work is licensed under a Creative Commons Attribution-NonCommercial-NoDerivatives 4.0 International License.

Lysosomal membrane permeabilization is involved in oxidative stress-induced apoptotic cell death in LAMP2-deficient iPSCs-derived cerebral cortical neurons

Cheuk-Yiu Law,[1] Chung-Wah Siu,[1,2] Katherine Fan,[3] Wing-Hon Lai,[1] Ka-Wing Au,[1] Yee-Man Lau,[1] Lai-Yung Wong,[1,2] Jenny C. Y. Ho,[1] Yee-ki Lee,[1] Hung-Fat Tse,[1,2] Kwong-Man Ng [1,2]

[1]Cardiology Division, Department of Medicine, Queen Mary Hospital, The University of Hong Kong, Hong Kong SAR, China; [2]Research Center of Heart, Brain, Hormone and Healthy Aging, Li Ka Shing Faculty of Medicine, The University of Hong Kong; Hong Kong SAR, China; [3] Cardiac Medical Unit, Grantham Hospital, Hong Kong SAR, China.

Correspondence to: **Kwong-Man Ng, PhD**

Department of medicine

Li Ka Shing Faculty of Medicine

The University of Hong Kong

L5-03, Laboratory Block, Faculty of Medicine Building, 21 Sassoon Rd. Hong Kong SAR, China

Tel: 852-3917-7559; Email: skykmng@hkucc.hku.hk

Abstract

Patients with Danon disease may suffer from severe cardiomyopathy, skeletal muscle dysfunction as well as varying degrees of mental retardation, in which the primary deficiency of lysosomal membrane-associated protein-2 (LAMP2) is considerably associated. Owing to the scarcity of human neurons, the pathological role of LAMP2 deficiency in neural injury of humans remains largely elusive. However, the application of induced pluripotent stem cells (iPSCs) may shed light on overcoming such scarcity.

In this study, we obtained iPSCs derived from a patient carrying a mutated *LAMP2* gene that is associated with Danon disease. By differentiating such LAMP2-deficient iPSCs into cerebral cortical neurons and with the aid of various biochemical assays, we demonstrated that the LAMP2-deficient neurons are more susceptible to mild oxidative stress-induced injury.

The data from MTT assay and apoptotic analysis demonstrated that there was no notable difference in cellular viability between the normal and LAMP2-deficient neurons under non-stressed condition. When exposed to mild oxidative stress (10 μM H_2O_2), the LAMP2-deficient neurons exhibited a significant increase in apoptosis. Surprisingly, we did not observe any aberrant accumulation of autophagic materials in the LAMP2-deficient neurons under such stress condition.

Our results from cellular fractionation and inhibitor blockade experiments further revealed that oxidative stress-induced apoptosis in the LAMP2-deficient cortical neurons was caused by increased abundance of cytosolic cathepsin L. These results suggest the involvement of lysosomal membrane permeabilization in the LAMP2 deficiency associated neural injury.

1. Introduction

Lysosomes are organelles responsible for the degradation of obsolete cellular constituents and cellular materials [1,2], and exist in virtually all eukaryotic cells. These organelles have long been regarded as merely trash cans; however, some latest reports demonstrated that they are involved in many vital cellular processes, including autophagy, plasma membrane repair and mediation of cell death [3,4].

Structurally, lysosomes are confined by individual phospholipid-bilayers whilst the lysosomal membrane contains specific sets of glycoproteins. The luminal domains of these proteins are usually highly glycosylated, so that they protect the lysosomal membranes against autolysis**.** Such unique membrane structures are important because injury of the lysosomal membrane may trigger the release of hydrolytic enzymes into the cytosol thus leading to apoptosis [5,6,7] or necrotic cell death [8].

To date, more than 20 lysosomal membrane proteins have been identified. Among them, lysosomal membrane-associated protein-1 and -2 (LAMP1 and LAMP2) are the most abundant. The functional roles of these two proteins are incompletely understood; yet, data from clinical and animal studies have suggested a direct association between LAMP2 and autophagy [9,10]. Accordingly to some previous clinical reports, LAMP2 deficiency led to Danon disease, which is a multisystem disorder associated with high morbidity and early mortality [11]. Aberrant accumulation of autophagic vacuoles had been observed in tissue samples of patients with Danon disease and LAMP2-deficient mice [4,8,12,13] suggesting that autophagy dysfunction is the plausible cause of cellular abnormality. To date, a number of reports acquainted the impact of

LAMP2 deficiency on the dysfunction of human cardiomyocytes; however, investigation of such deficiency on neural defects is rather limited. We believe the scarcity of source and difficulties in cultural maintenance largely restrained the studies of pathological significance of LAMP2 deficiency on human neurons.

With the latest development of the induced pluripotent stem cell (iPSC) technology, patient specific-iPSCs can now be efficiently differentiated into various cell types such as cardiomyocytes and cortical neurons [14,15]. To this end, such technology provides an authentic human cell-based platform for modeling various inheritable disorders. Recently, we have identified from members of a Chinese family a novel *LAMP2* (c.183_184insA) mutation that is associated with severe cardiomyopathy. Although cardiomyopathy is the leading cause of death in patients with primary LAMP2 deficiency [13], mental retardation is often observed in many of these patients [16,17,18]. As such, the iPSCs generated from the patients with *LAMP2* mutation represent a powerful tool for evaluating the pathophysiological mechanisms of LAMP2-deficiency and the associated multiple system disorders, particularly related to the c.183_184insA mutation of the *LAMP2* gene.

With the advent of iPSC technology, we and many other research groups are determined to investigate the association between LAMP2 deficiency and cardiac disorders, as well as the pathophysiological mechanism underlying *LAMP2* mutations and neural dysfunction. In the present study, we successfully generated LAMP2-deficient iPSCs from a male patient and differentiated them into cerebral cortical neurons for disease modeling. This study is the first to report that the LAMP2-deficient human neurons are more susceptible to oxidative stress-induced

apoptotic cell death and such apoptotic mechanism was associated with an increased lysosomal membrane permeabilization (LMP).

2. Materials and Methods

2.1. Patient

The patient sample of this study has been described previously [13]. In brief, the cardiac biopsies were obtained from a 17-year-old male, designated Patient II-1, who showed left ventricular hypertrophic pattern and diffused deep symmetrical T inversion. He was diagnosed with Danon disease rooted from the lack of LAMP2 protein production. From his cardiac biopsies, an insertion of "A" residue between the 183th and 184th position of the *LAMP2* gene was identified by means of the detailed genomic DNA sequencing analysis. For this reason, this mutation will be denoted as *LAMP2-c.183_184insA* in this article. The sequencing analysis indicated that this mutation created multiple stop codons downstream of the affected region. As a result, any polypeptides translated from this allele were predicted to be extremely short.

2.2. Generation of LAMP2-deficient iPSCs

The protocol for the procurement of human tissue for use in our reprogramming experiments of this study was approved by the Institutional Review Board of Queen Mary Hospital, Hong Kong, and was registered at the Clinical Trial Center (HKCTR-725), The University of Hong Kong, (http://www.hkclinicaltrials.com). Written informed consents had been obtained from all participants. The detailed procedures of iPSCs generation from patient biopsy have been described previously [14,19]. In Brief, skin biopsies were performed, from which dermal

fibroblasts were collected and expanded accordingly in Dulbecco's Modified Eagle Medium (DMEM, Gibco) supplemented with 10% fetal bovine serum (FBS, Gibco). Skin fibroblasts were cultured in 6-well plates at a density of 1×10^5 cells/well, and infected with a cocktail of retrovirus packaged with Yamanaka's 4 factors, human Sox2, Klf4, Oct4 and c-Myc [20]. Putative iPSCs-like clones were selected manually and expanded with feeder-free systems in StemPro hESC medium (Gibco) in Geltrex-coated plates. Authenticity of iPSCs was determined by means of standard characterization methods such as pluripotency marker expression analysis, Nanog promoter analysis and *in vivo* teratoma formation (for details, please refer to Supp. Fig. 1). To minimize clone-to-clone variation, data collected in the present study were derived from more than 3 individual clones of the patient derived iPSCs. In addition, the well characterized iPSC line KS1, [19] which was generated from a healthy male individual, was used as the control in the present study.

2.3. Neural induction

The differentiation of iPSCs into cerebral cortical neurons was performed according to a published protocol [15] with modifications. In brief, iPSC colonies were dissociated into single cells using accutase and cultured in Matrigel-coated 12-well plates at a density of 7.5×10^5 cells/well. These dissociated cells were maintained in TeSR™-E8™ medium (STEMCELL Technologies, USA) and supplemented with 10 µM Y-27632 for an enhancement of cell viability. When cells reached 100% confluence, neural differentiation was induced by switching to a neural induction medium [DMEM/F-12 medium (Gibco) supplemented with noggin (500 ng/mL, Sigma-Aldrich), SB 431542 (10 µM, Sigma-Aldrich), 0.5 X N-2 supplement (Gibco), 2-mercaptoethanol (50 µM, Gibco), 0.5 X B-27 supplement (Gibco) and insulin (5 µg/mL, Sigma-

Aldrich)]. Neural induction medium was replaced every day for 14 days until the formation of uniform neuroepithelial sheets. The neuroepithelial sheet was passed onto Matrigel-coated 6-well plates and cultured in neural induction medium supplemented with 10 µM Y-27632 for 1 day. Thereafter, the induced cells were maintained in neural maintenance medium (neural induction medium without noggin and SB 431542). Once the neural rosettes became observable (around 17 days after induction), the culturing medium was supplemented with fibroblast growth factor-2 (FGF2, 20 ng/mL) for neural expansion. The differentiated neurons were ready for experiments after 2-3 passages.

2.4. Cardiac Differentiation

Differentiations of iPSCs into cardiomyocytes were performed using the commercial PSC-Cardiomyocyte Differentiation Kit (Gibco). In brief, monolayers of iPSCs were prepared following the methods previously described in section 2.3. At 70% confluency, the spent medium was replaced with Cardiomyocyte Differentiation Medium A provided in the differentiation kit and cultured for 2 days. Next, spent medium was replaced with Cardiomyocyte Differentiation Medium B and the differentiating cells were cultured for additional 2 days. Subsequently, dead cells were washed out with 1X PBS and the differentiating cells were kept culturing in Cardiomyocyte Maintenance Medium provided in the differentiation kit until the appearance of beating cardiomyocytes (about 14 days after the initiation of cardiac differentiation). In the meantime, spent medium was refreshed every 2-3 days.

2.5. Oxidative stress induction and cathepsin L inhibition

To induce oxidative stress, iPSCs-derived neurons were treated with different concentrations of hydrogen peroxide (H_2O_2, Sigma-Aldrich). Unless stated specifically, the time for H_2O_2

treatment was 24 hour. When necessary, cathepsin L specific inhibitor was added as an anti-oxidative stress agent.

2.6. Antibodies

Monoclonal antibodies specific to Nanog (09-0020), Oct-4 (09-0023). SSEA-4 (09-0006) and TRA-1-60 (09-0010) were purchased from Stemgent. Monoclonal antibodies specific to LAMP1 (14-1079) and LAMP2 (14-1078) were purchased from eBioscience. Monoclonal antibody specific to cathepsin L (C4618) was purchased from Sigma-Aldrich. Monoclonal antibodies specific to MAP2 (8707) were purchased from cell signaling technology. Polyclonal antibody specific to N-terminal of LAMP2 (sc-5571) and monoclonal antibody specific to β-ACTIN (sc-47778) were purchased from Santa Cruz biotechnology.

2.7. Cell lysis and Western blot analysis

iPSCs-derived neurons were harvested by scraping and cell pellets were collected by centrifugation. For total protein isolation, cells were lysed with RIPA buffer (Sigma-Aldrich) supplemented with protease inhibitor cocktail (Sigma-Aldrich). Cell debris was removed by centrifugation and the supernatant was saved. The cytosolic fraction, when needed, was isolated using the subcellular protein fractionation Kit (Thermo Scientific) following the manufacturer's instruction. For Western blot analysis, 25-40 µg of total or cytosolic protein samples were resolved on 4-12 % Bolt® Bis-Tris Plus gels (Invitrogen, USA) and transferred onto PVDF membranes using the iBlot® system (Invitrogen). The membranes were then blocked with Tris-buffered saline (TBS) containing 5 % non-fat dry milk and 0.05% Tween-20 for 1 hour at room temperature. Afterwards, membranes were incubated with appropriate primary antibodies at 4 ^{o}C

for 16 hr. Unbound antibodies were removed by three washes with washing buffer (TBS containing 0.05% Tween-20) followed by the incubation of HRP-conjugated secondary antibodies. Unbound secondary antibodies were removed by three washes with washing buffer and the immunoreactive proteins were detected using the Amersham ECL Prime Western Blotting Detection Reagent (GE Healthcare Life Science).

2.8. Immunofluorescence staining

Immunofluorescence staining was performed according to the method described previously [21]. In brief, iPSCs-derived neurons were fixed with 2 % paraformaldehyde for 10 minutes at room temperature, washed with phosphate-buffered saline (PBS) and permeabilized with PBS containing 0.05 % Triton-X 100 (PBS-T) for 10 minutes at room temperature. Cells were then incubated with appropriate primary antibodies at 4 ^{o}C overnight. Unbound antibodies were removed by 3 washes with PBS and neurons were incubated with alexa fluor-conjugated secondary antibodies (Alexa 488 or Alexa 647) for 30 minutes. The samples were mounted with ProLong® Gold Antifade Mountant with DAPI (life technology) and examined under the Olympus fluorescence microscope.

2.9. Cell viability assay

The iPSCs-derived neurons were firstly seeded in 96-well plates with 200 µl of neural maintenance medium at a density of 1×10^4 cells/well at 37 °C for 48 hours to allow growth and even attachment. Thereafter, the cells were exposed to different concentrations of H_2O_2 in the presence or absence of cathepsin-L inhibitor for 24 hr. Afterward, 3-(4,5-dimethylthiazol-2-yl)-2,5-diphenyltetrazolium bromide (MTT) solution (10 µl) was added into each well. After the 4-hr

incubation at 37 °C, the wells were drained and DMSO solution (100 µl) was added into each well to dissolve the formazan. The absorbance at wavelength 540 nm was measured using a microplate reader.

2.10. TUNEL assay

The apoptotic status of the iPSC-derived neurons was evaluated using the APO-BrdU™ TUNEL Assay Kit (Life tech., USA). Experiments were performed following the manufacturer's instruction, in brief, the iPSC-derived neurons were dissociated with accuses and collected by centrifugation. Cell pellets were re-suspended in PBS and fixed with 4% paraformaldehyde on ice for 15 min. Paraformaldehyde was removed by centrifuging and the cell pellets were washed with PBS twice. Afterwards, cell pellets were re-suspended in PBS and ice-cold 70 % ethanol was added to each sample. The cell suspension was then incubated overnight at -20 ^{o}C. The damaged DNA in the samples were labelled with DNA-labelling solution (10 µL reaction buffer, 0.75 µl TdT enzyme, 8.0 µl BrdUTP and 3.75 µl distilled water) and incubated at 37°C for 1 hr. After incubation, the samples were washed twice with rinse buffer. Then, washed samples were incubated with Alexa Fluor-488-labeled anti-BrdU antibody solution at room temperature for 30 min. The percentages of apoptotic cells were determined by flow cytometry.

2.11. Caspase-3/7 activity assay

The percentage of cells containing active caspase-3/7 was evaluated using the CellEvent® Caspase-3/7 green detection reagent (Invitrogen). Experiments were performed according to the manufacturer's instruction. In brief, iPSC-derived neurons were cultured on glass coverslips and treated with H_2O_2 at 37 ^{o}C for 24 hr. Cathepsin L-inhibitor was used as a positive control.

Thereafter, the detection reagent was applied to each sample at the concentration of 2 drops / 1 ml medium. The cells were then incubated with the detection reagent at 37 ^{o}C for 30 min. The samples were then examined under a fluorescence microscope of a live cell imaging system (name of the microscope). When needed, the cells were fixed with paraformaldehyde for an additional immunostaining analysis.

2.12. Periodic Acid-Schiff (PAS) Staining

The intracellular accumulation of glycogen was evaluated using the Periodic Acid-Schiff (PAS) staining kit (Sigma-Aldrich) following the manufacturer's instruction. In Brief, iPSC-derived neurons were cultured on gelatin-coated glass coverslips, fixed with 1% paraformaldehyde for 10 min and equilibrated in PBS prior to the staining procedures. To start the staining, fixed cells were immersed in periodic acid solution for 5 min at room temperature. The cells were then rinsed 5 times with distilled water and immersed in Schiff's reagent for 15 min at room temperature. Reaction was stopped by rinsing the cells in running tap water for 5 min. After that, slides were counterstained with hematoxylin solution and examined under a light microscope.

2.13. Acridine Orange staining

Acridine orange was purchased from Thermo Scientific, and the staining procedure was performed following the instructions provided by the manufacturer. In brief, cells of interest were cultured in confocal dishes. At confluence of 40-60%, the cells were incubated with acridine orange solution (5 μg/ml, diluted in culture medium) at 37^{o}C for 10 min. Acridine orange-stained cells were washed 3 times with normal culture medium, and examined using the Olympus fluorescence microscope.

2.14. Statistical analysis

Continuous variables are expressed as mean ± SEM. Statistical comparisons between two groups

were performed using Student's *t* test. One-way ANOVA or two-way ANOVA analyses were used for comparing more than 2 groups. For one-way ANOVA analysis, Tukey post-hoc test was used to compare all pairs of columns. For two-way ANOVA analysis, Bonferroni post-hoc tests were performed to compare the replicated means. Calculations were performed with the GraphPad Prism 5 (GraphPad). $P < 0.05$ was considered statistically significant.

3. Results

3.1 *LAMP2-c.183_184insA* mutation abolished LAMP2 production

Recently, we have reported a *LAMP2* mutation associated Danon disease from members of a Hong Kong family suffered from severe cardiomyopathy (Fig. 1A). This specific mutation involves a single nucleotide (A) insertion at the coding sequence region of exon 3 of the *LAMP2* gene (Fig. 1B). Sequencing analysis indicated that such insertion creates multiple stop codons downstream of the affected region (Fig. 1C), as such, any polypeptides translated from the affected alleles were estimated to be very short (about 8.6 kDa) and unlikely to be functional. To investigate the existence of these short truncated proteins, total proteins extracted from the skin fibroblasts were examined by means of Western Blot analysis. By using a polyclonal antibody specific for the N-terminal region of the human LAMP2 protein, we observed that the majority of the immunoreactive proteins detected from the wildtype LAMP2 samples (Fig. 1D) were about 120 kDa, or so-called the full-length form. Our observation was in agreement with published reports of other research groups [22,23,24] and the difference between the observed size and the size deduced from the amino acid sequencing is likely due to the glycosylation of the protein [22]. In addition, a trace amount of immunoreactive protein of about 60 kDa was obtained from the LAMP2-deficient samples. To address whether this truncated protein was derived from alternative *LAMP2* transcript(s) or from differential glycosylation, further studies

will be desperately needed. On the other hand, we were not able to detect any LAMP2-immunoreactive signal in the total protein isolated from the biopsy of Patient II-1 even we increased the loading amount of protein to 40 µg. Similar results were observed from the patient's iPSCs, no immunoreactive LAMP2 protein were detected in immunostaining or Western blot analysis (Fig. 1E and F). These observations were in line with our previous report that no immunoreactive LAMP2 was detected in the cardiac biopsy of the same patient [13]. Based on these observations, we believe that any polypeptides translated from the mutant *LAMP2* allele are highly susceptible to degradation and do not accumulate within the cell. As such, in the following sections, the iPSCs and the neurons derived from Patient II-1 were denoted as LAMP2-defeicient iPSCs or LAMP2-deficient neurons respectively.

3.2. LAMP2 expression was diminished in LAMP2-deficient iPSCs-derived cortical neurons

Mental retardation is often observed in patients with Danon disease. To investigate the direct effect of LAMP2 deficiency on the brain, we adopted the specific protocols to generate cerebral cortical neurons for better recapitulation of the diseased condition. As shown in Supplementary Figure 2, uniform neuroepithelial sheets began to form about 2 weeks after the start of induction. In approximately 60 days, the iPSCs-derived neurons were ready for experiments. At this stage, over 70% of the iPSCs were MAP2-positive in both control and LAMP2-deficient neurons indicating that the cells were efficiently differentiated into neurons (Supplementary Fig. 2). By means of immunostaining and Western Blot analysis, we examined the LAMP2 protein levels in those iPSCs-derived neurons. As showed in Fig. 2A, in the control groups, most LAMP2 proteins were primarily distributed around the perinuclear and cell body regions, though the abundance of LAMP2 in the axon regions was not obvious. On the contrary, no LAMP2 signal

was detected in the LAMP2-deficient neurons. Similar results were observed in our Western Blot analysis (Fig. 2A, right panel).

3.3. LAMP2-deficient neurons were more susceptible to oxidative stress-induced apoptosis

In order to compare the viabilities of the cortical neurons derived from control iPSCs and LAMP2-deficient iPSCs, MTT assays were performed. As shown in Fig. 2B, under non-stress condition, there was no significant difference in cell viability between the two groups. However, when subjected to mild oxidative stress (10 μM H_2O_2), the LAMP2-deficient neurons exhibited a significant reduction in viability (about 50%, $P<0.001$), while the normal neurons only showed a slight reduction. On the other hand, when exposed to strong oxidative stress (30 and 50 μM H_2O_2), substantial cell death (over 90%) was observed in both normal and LAMP2-deficient neurons. According to some previous studies, mild oxidative stress resulted in apoptosis while severe oxidative stress triggered necrosis [25]. Therefore, we focused on the apoptotic status of the iPSCs-derived neurons under a mild oxidative stress condition. As revealed by TUNEL assay, the apoptotic index in the LAMP2-deficient neurons were significantly higher than the normal neurons (6-fold increase, $P<0.001$) (Fig. 2C). To further confirm the occurrence of apoptosis, we evaluated the caspase-3/7 activities in the iPSCs-derived neurons. As showed in Fig. 2D, the ratio of activated caspase-3/7 to MAP2-positive (cortical neurons) cells was significantly higher in the LAMP2-deficient group subjected to 10 μM H_2O_2 treatment although each group exhibited a certain amount of caspase-3/7 activity. These results suggested that the LAMP2 deficiency rendered the iPSCs-derived cortical neurons more susceptible to mild oxidative stress-induced apoptosis.

3.4. Oxidative stress-induced apoptotic cell death in LAMP2-deficient iPSCs-derived cortical neurons was mediated by Cathepsin L

The association between LAMP2 deficiency and autophagy impairment has been well documented. In our previous study, we had observed abnormal accumulation of glycogen granules and autophagosomes in the cardiac biopsy of Patient II-1 [13]. As such, we suspected similar pathophysiological phenotype would be observed in the iPSCs-derived neurons from Patient II-1. However, according to the PAS staining result, we were unable to observe any abnormal accumulation of glycogen granules in the LAMP2-deficient iPSCs-derived neurons (Fig. 3A, left panel). In the iPSCs-derived cardiomyocytes from the same patient, aberrant glycogen accumulation, as indicated by the deposition of deep pink stain, was evidently observed. (Fig. 3A, right panel). In addition, we had also examined the presence of autophagosome in the iPSCs-derived cortical neurons by means of immunostaining analysis. Regardless of the presence of mild oxidative stress (10 μM H_2O_2), no identifiable accumulation of LC3-positive punctae was observed in all sample groups (Fig. 3B). Based on this observation, we speculated that the oxidative stress-induced apoptosis was mediated by LMP under the deficiency of LAMP2. To test this hypothesis, we first evaluated the leakage of lysosomal contents using acridine orange staining. In the control neurons, the occurrence of bright red punctae indicated the acidic contents were well enclosed in intracellular compartments, such as endosomes and lysosomes (Fig. 3C). On the contrary, the red fluorescents were more dispersed and no obvious punctae was noted in the LAMP2-deficint neurons. This result suggests that the acidic contents were released from the endosomes or lysosomes into the cytosol. In the light of this observation, we further studied the subcellular distribution of lysosomal enzymes, particularly cathepsins, in the cytosolic fractions of the iPSCs-derived neurons by means of Western blotting analysis. As shown in Fig. 4A, we observed an up-regulated production of both pro-cathepsin L (42 kDa) and

active cathepsin L (25 kDa) in the LAMP2-deficient iPSCs-derived neurons, but not cathepsins B or D. More specifically, the active form of cathepsin L (25 kDa) was only detected in the cytosolic sub-fraction of the LAMP2-deficient neurons. When exposed to oxidative stress, a significant increase (1.8-fold, $P<0.05$) of cytosolic cathepsin L was observed in the LAMP2-deficinet neurons whilst a relatively low level of cytosolic cathepsin L was detected in the normal control (Fig. 4B). Taken together, these results supported our hypothesis that the oxidative stress-induced apoptosis was mediated by LMP under the deficiency of LAMP2.

3.5. Cathepsin L-specific inhibitor protected the LAMP2-deficient iPSCs-derived neurons from mild oxidative stress

In order to confirm the pathological association between the presence of cytosolic cathepsin L and oxidative stress-induced apoptosis in the LAMP2-deficient neurons, we repeated the experiments with the addition of a cathepsin L specific inhibitor (RKLLW-NH_2) [26]. As shown in Fig. 5A, the application of cathepsin L inhibitor remarkably increased the viability of the LAMP2-deficient neurons when exposed to H_2O_2 (10 μM). In particular, the application of cathepsin L inhibitor at 30 μM almost restored the relative viability (compared with the groups without H_2O_2 treatment) to 80% ($P<0.001$), and the average percentages of oxidative stress-induced apoptotic neurons were reduced from nearly 45% to about 4.5 % ($P<0.01$, Fig. 5B). Similarly, the average percentages of caspase-3/7-activated neurons were also significantly reduced from about 43% to 24% ($P<0.001$, Fig. 5C). These results indicated that the oxidative stress-induced apoptosis in the LAMP2-deficient neurons was mediated by cathepsin L.

4. Discussion

This report is the first to demonstrate that cortical neurons derived from LAMP2-deficient human iPSCs are more susceptible to oxidative stress-induced apoptosis and such apoptotic cell death is negatively regulated by cytosolic cathepsin L.

The pathological significance of LAMP2 deficiency has been well documented. According to clinical studies, the mutations in *LAMP2* genes are associated with the X-linked Danon disease. It is now clear that Danon disease is a multisystem disorder that characterized by severe cardiomyopathies, skeletal muscles dysfunctions, hepatic dysfunctions as well as mental retardation. Probably due to the fact that cardiomyopathies are the leading cause of death in Danon disease, most studies have been focused on the cardiac manifestations while studies on the pathological roles of *LAMP2* mutations in non-cardiac tissues are very limited. With the increasing success in cardiac transplantation operations, those non-cardiac symptoms conversely may turn to be clinical issues since the post-operational life of the patient is largely affected.

In this study, we attempted to create a patient-specific iPSCs-based model for evaluating the pathological roles of LAMP2 deficiency in cortical neurons, so as to provide clinical insights on Danon disease associated mental retardation. Comparable to the normal control, the LAMP2-deficient cortical neurons appeared to be grossly viable under non-stressed condition. However, when they were subjected to mild levels of oxidative stress (H_2O_2, 10 μM), a significant increase in cell death was observed. Further analyses revealed that such oxidative stress-induced cell death was correlated with the increases in caspase-3/7 activity and apoptotic signal.

The association between LAMP2 deficiency and autophagy dysfunction has been well documented [10,27,28], meanwhile, there is also a strong interrelationship between autophagy and apoptosis [27,29]. As such, the oxidative stress-induced apoptosis in the LAMP2-deficient neurons could be a result of autophagy impairment. In fact, we had previously demonstrated the abnormal accumulation of glycogen granules and autophagic materials in the cardiac biopsy of the same patient (Patient II-1) [13]. In this study, increased glycogen accumulation was again observed in the LAMP2-deficient cardiomyocytes of the same patient. However, to our surprise, no aberrant accumulation of glycogens or LC3-positive vesicles was obtained in the LAMP2-deficient iPSC-derived neurons of this patient. The exact reason for this observation remains to be elucidated, but we speculated that it may be due to the different metabolic activities in cardiomyocytes and neurons.

When the cells were treated with H_2O_2 (10 μM), a trace amount of active cathepsin L became detectable in the cytosols of normal controls; however, the levels of cytosolic active cathepsin L were increased by almost 2 folds in the LAMP2-deficient neurons. The excessive generation of reactive oxygen species is known to cause lipid peroxidation and lead to the damage of lysosomal membrane [30]; however, healthy cells and tissues are usually able to combat mild oxidative stress in the presence of intrinsic antioxidant defense mechanisms [31]. Nevertheless, in the absence of LAMP2, the lysosomal membrane integrity is plausibly reduced and becomes more susceptible to oxidative stress thus leading to lysosomal leakage. For example, oncogene-induced down-regulation of LAMP1 and LAMP2 was found to increase lysosomal membrane permeability and sensitize the lysosomal cell death pathway [32].

Although both lysosomal acid hydrolase and lysosomal cathepsins may contribute to lysosomal cell death, results from various study suggest that cathepsins are the major carriers of lysosomal cell death pathway many [33]. For example, in a rat model, application of cathepsin inhibitors was shown to reduce neuronal damage-induced ischemic insults [34]. Similar to this finding, our result also demonstrated that the application of cathepsin L-specific inhibitor significantly reduced the apoptosis in the LAMP2-deficient neurons treated with H_2O_2 (10 μM). This clearly demonstrated that cathepsin L is a key mediator of mild oxidative stress-induced apoptosis in the LAMP2-deficient neurons. Conversely, the transient increase of intra-lysosomal cathepsin L activity has also been implicated in the neuronal death induced by serum and potassium deprivation [35]. Nevertheless, the LAMP2-deficient neurons showed certain degree of lysosomal leakage even in the absence of oxidative stress. In this regard, we suggest that the differential susceptibility between the normal and LAMP2-deficient neurons to oxidative stress is likely due to the increased release of lysosomal cathepsin L into the cytosol.

In summary, our study provided an important evidence for the involvement of LMP in the oxidative stress-induced neuronal cell death associated with LAMP2 deficiency. In the past decades, autophagy dysfunction was suggested to be the major pathological pathway associated with Danon disease. In the aspect of diagnosis, the excessive accumulation of autophagic vesicles and glycogen granules are relatively easy to identify; nevertheless, how the accumulation of these materials directly causes cell death remains unclear. In this regard, our results provided a concrete evidence for the presence of a non-autophagy mechanism that may help to explain the direct effects of LAMP2 deficiency on the neuronal susceptibility to oxidative stress.

In this study, we have been focused on the cortical neuron models, however, increasing evidences have pointed out the improvement of cathepsin L in the progression of myopathy. Thus, it would also be interesting to evaluate the involvement of the lysosomal cell death pathway in the cardiomyocytes derived from the LAMP2-deficient iPSCs, and we are currently setting a pilot work on such study.

Acknowledgements

We would like to sincerely thank Dr. S.W. Tsang (Hong Kong Baptist University) for her assistance in providing professional English editing services.

Funding

This work was supported by the Hong Kong Research Grant Council: Theme Based Research Scheme (T12-705/11) and General Research Fund (HKU 775613); Innovation and Technology Support Programme (Tier 3) (ITS/303/12); and The University of Hong Kong: Seed Funding Programme for Basic Research (201411159002)

References

[1] F. Appelmans, R. Wattiaux, C. De Duve, Tissue fractionation studies. 5. The association of acid phosphatase with a special class of cytoplasmic granules in rat liver, Biochem J 59 (1955) 438-445.

[2] M. Baggiolini, C. de Duve, M. Klockars, Lysosomes, Scand J Rheumatol Suppl 12 (1975) 144-148.

[3] P.A. Kreuzaler, A.D. Staniszewska, W. Li, N. Omidvar, B. Kedjouar, J. Turkson, V. Poli, R.A. Flavell, R.W. Clarkson, C.J. Watson, Stat3 controls lysosomal-mediated cell death in vivo, Nat Cell Biol 13 (2011) 303-309.

[4] H. Appelqvist, P. Waster, K. Kagedal, K. Ollinger, The lysosome: from waste bag to potential therapeutic target, J Mol Cell Biol 5 (2013) 214-226.

[5] K. Roberg, K. Kagedal, K. Ollinger, Microinjection of cathepsin d induces caspase-dependent apoptosis in fibroblasts, Am J Pathol 161 (2002) 89-96.

[6] C.A. Bivik, P.K. Larsson, K.M. Kagedal, I.K. Rosdahl, K.M. Ollinger, UVA/B-induced apoptosis in human melanocytes involves translocation of cathepsins and Bcl-2 family members, J Invest Dermatol 126 (2006) 1119-1127.

[7] O. Schestkowa, D. Geisel, R. Jacob, A. Hasilik, The catalytically inactive precursor of cathepsin D induces apoptosis in human fibroblasts and HeLa cells, J Cell Biochem 101 (2007) 1558-1566.

[8] W. Li, X. Yuan, G. Nordgren, H. Dalen, G.M. Dubowchik, R.A. Firestone, U.T. Brunk, Induction of cell death by the lysosomotropic detergent MSDH, FEBS Lett 470 (2000) 35-39.

[9] P. Saftig, W. Beertsen, E.L. Eskelinen, LAMP-2: a control step for phagosome and autophagosome maturation, Autophagy 4 (2008) 510-512.

[10] R. Ruivo, C. Anne, C. Sagne, B. Gasnier, Molecular and cellular basis of lysosomal transmembrane protein dysfunction, Biochim Biophys Acta 1793 (2009) 636-649.

[11] D. Boucek, J. Jirikowic, M. Taylor, Natural history of Danon disease, Genet Med 13 (2011) 563-568.

[12] K. Roberg, K. Ollinger, Oxidative stress causes relocation of the lysosomal enzyme cathepsin D with ensuing apoptosis in neonatal rat cardiomyocytes, Am J Pathol 152 (1998) 1151-1156.

[13] A.K. Ng, K.M. Ng, H.F. Tse, W.H. Lai, W.S. Chan, C.W. Siu, K. Fan, Pseudo-pre-excitation unraveled down to its core, Circulation 130 (2014) e56-58.

[14] H.F. Tse, J.C.Y. Ho, S.W. Choi, Y.K. Lee, A.W. Butler, K.M. Ng, C.W. Siu, M.A. Simpson, W.H. Lai, Y.C. Chan, K.W. Au, J.Q. Zhang, K.W.J. Lay, M.A. Esteban, J.M. Nicholls, A. Colman, P.C. Sham, Patient-specific induced-pluripotent stem cells-derived cardiomyocytes recapitulate the pathogenic phenotypes of dilated cardiomyopathy due to a novel DES mutation identified by whole exome sequencing, Human Molecular Genetics 22 (2013) 1395-1403.

[15] Y. Shi, P. Kirwan, F.J. Livesey, Directed differentiation of human pluripotent stem cells to cerebral cortex neurons and neural networks, Nat Protoc 7 (2012) 1836-1846.

[16] M.J. Danon, S.J. Oh, S. DiMauro, J.R. Manaligod, A. Eastwood, S. Naidu, L.H. Schliselfeld, Lysosomal glycogen storage disease with normal acid maltase, Neurology 31 (1981) 51-57.

[17] M. Fanin, A.C. Nascimbeni, L. Fulizio, M. Spinazzi, P. Melacini, C. Angelini, Generalized lysosome-associated membrane protein-2 defect explains multisystem clinical involvement and allows leukocyte diagnostic screening in Danon disease, Am J Pathol 168 (2006) 1309-1320.

[18] Z. Yang, C.J. McMahon, L.R. Smith, J. Bersola, A.M. Adesina, J.P. Breinholt, D.L. Kearney, W.J. Dreyer, S.W. Denfield, J.F. Price, M. Grenier, N.J. Kertesz, S.K. Clunie, S.D. Fernbach, J.F. Southern, S. Berger, J.A. Towbin, K.R. Bowles, N.E. Bowles, Danon disease as an underrecognized cause of hypertrophic cardiomyopathy in children, Circulation 112 (2005) 1612-1617.

[19] W.H. Lai, J.C. Ho, Y.K. Lee, K.M. Ng, K.W. Au, Y.C. Chan, C.P. Lau, H.F. Tse, C.W. Siu, ROCK inhibition facilitates the generation of human-induced pluripotent stem cells in a defined, feeder-, and serum-free system, Cell Reprogram 12 (2010) 641-653.

[20] K. Takahashi, K. Tanabe, M. Ohnuki, M. Narita, T. Ichisaka, K. Tomoda, S. Yamanaka, Induction of pluripotent stem cells from adult human fibroblasts by defined factors, Cell 131 (2007) 861-872.

[21] K.M. Ng, Y.C. Chan, Y.K. Lee, W.H. Lai, K.W. Au, M.L. Fung, C.W. Siu, R.A. Li, H.F. Tse, Cobalt chloride pretreatment promotes cardiac differentiation of human embryonic stem cells under atmospheric oxygen level, Cell Reprogram 13 (2011) 527-537.

[22] J.W. Chen, G.L. Chen, M.P. D'Souza, T.L. Murphy, J.T. August, Lysosomal membrane glycoproteins: properties of LAMP-1 and LAMP-2, Biochem Soc Symp 51 (1986) 97-112.

[23] M. Fukuda, J. Viitala, J. Matteson, S.R. Carlsson, Cloning of cDNAs encoding human lysosomal membrane glycoproteins, h-lamp-1 and h-lamp-2. Comparison of their deduced amino acid sequences, J Biol Chem 263 (1988) 18920-18928.

[24] S.R. Carlsson, M. Fukuda, The polylactosaminoglycans of human lysosomal membrane glycoproteins lamp-1 and lamp-2. Localization on the peptide backbones, J Biol Chem 265 (1990) 20488-20495.

[25] M.B. Hampton, S. Orrenius, Dual regulation of caspase activity by hydrogen peroxide: implications for apoptosis, FEBS Lett 414 (1997) 552-556.

[26] A. Brinker, E. Weber, D. Stoll, J. Voigt, A. Muller, N. Sewald, G. Jung, K.H. Wiesmuller, P. Bohley, Highly potent inhibitors of human cathepsin L identified by screening combinatorial pentapeptide amide collections, Eur J Biochem 267 (2000) 5085-5092.

[27] A.M. Cuervo, E. Wong, Chaperone-mediated autophagy: roles in disease and aging, Cell Res 24 (2014) 92-104.

[28] Z. Yang, M. Vatta, Danon disease as a cause of autophagic vacuolar myopathy, Congenit Heart Dis 2 (2007) 404-409.

[29] Y. Uchiyama, Autophagic cell death and its execution by lysosomal cathepsins, Arch Histol Cytol 64 (2001) 233-246.

[30] A.C. Johansson, H. Appelqvist, C. Nilsson, K. Kagedal, K. Roberg, K. Ollinger, Regulation of apoptosis-associated lysosomal membrane permeabilization, Apoptosis 15 (2010) 527-540.

[31] B. Halliwell, Antioxidant defence mechanisms: from the beginning to the end (of the beginning), Free Radic Res 31 (1999) 261-272.

[32] N. Fehrenbacher, L. Bastholm, T. Kirkegaard-Sorensen, B. Rafn, T. Bottzauw, C. Nielsen, E. Weber, S. Shirasawa, T. Kallunki, M. Jaattela, Sensitization to the lysosomal cell death pathway by oncogene-induced down-regulation of lysosome-associated membrane proteins 1 and 2, Cancer Res 68 (2008) 6623-6633.

[33] S. Aits, M. Jaattela, Lysosomal cell death at a glance, J Cell Sci 126 (2013) 1905-1912.

[34] J.A. Windelborn, P. Lipton, Lysosomal release of cathepsins causes ischemic damage in the rat hippocampal slice and depends on NMDA-mediated calcium influx, arachidonic acid metabolism, and free radical production, J Neurochem 106 (2008) 56-69.

[35] A. Kaasik, T. Rikk, A. Piirsoo, T. Zharkovsky, A. Zharkovsky, Up-regulation of lysosomal cathepsin L and autophagy during neuronal death induced by reduced serum and potassium, Eur J Neurosci 22 (2005) 1023-1031.

Figure Legends

Figure 1 *LAMP2-C.183_184insA* mutation abolished the production of LAMP2 protein. (**A**) Pedigree information about members of a Hong Kong family carrying the Danon disease associated *LAMP2* mutations. (**B**) Detection of an insertion of A in the exon 3 of the *LAMP2* gene by means of genomic DNA sequencing analysis. (**C**) Outline of the predicted amino acid sequences of the normal and mutant LAMP2 polypeptides. The affected coding regions are highlighted in yellow whereas the stop codons are highlighted in red. The red arrow indicates the start of the affected area in the mutant. (**D**) Western blot analysis using an antibody specific to the N-terminal of LAMP2. The absence of LAMP2 protein production in the skin fibroblasts derived from Patient II-1 was confirmed. (**E and F**) The absence of LAMP2 protein production in the iPSCs-generated from Patient II-1 was confirmed by immunostaining and Western blot analysis.

Figure 2 LAMP2-deficient iPSCs-derived cortical neurons were more susceptible to apoptotic cell death induced with 10 μM H_2O_2. (**A**) Immunostaining (right panel) and Western blot analysis (left panel) confirmed that the cortical neurons derived from Danon disease patient-specific-iPSCs were deficient in LAMP2 production. Scale bar: 20 μm. (**B**) MTT assay was used to evaluate the viability of the iPSCs-derived cortical neurons under different concentrations of H_2O_2. n = 4 for each group. ***: P<0.001 comparing to the non-treated group of the same cell line, ###: P<0.001 comparison between the groups receiving 10 μM H_2O_2 treatment. (**C**) Flow cytometric analysis of the iPSCs-derived cortical neurons treated with 10 μM H_2O_2, the basal value obtained from the group receiving 0 μM H_2O_2 treatment was assigned as 0% apoptosis. n = 4 for each group, ***:P<0.001 (**D**) The percentage of activated caspase-3/7 cells were evaluated with the CellEvent Caspase-3/7 Green Detection Reagent. Scale bar: 40 μm. n = 1000 cells from 3-7 fields for each group, ***: P<0.001 comparing to the normal neurons treated with 0 μM H_2O_2, ###: P<0.001 comparing to the LAMP2-deficient neurons treated with 0 μM H_2O_2.

Figure 3. LAMP2-deficient neurons showed no obvious accumulation of autophagy materials but exhibited increased levels of cytosolic cathepsin-L. (**A**) PAS staining revealed no observable accumulation of glycogen granules (dark pink stain) in both normal and LAMP2-deficient iPSCs-derived cortical neurons and cardiomyocytes. Scale bar: 40 μm (**B**) Co-immunostaining analysis indicated that H_2O_2 (10 μM) treatment did not cause accumulation of LC3-positive vesicles in both normal and LAMP2-deficient iPSCs-derived cortical neurons. Scale bar: 20 μm. (**C**) Acridine orange staining revealed the increased leakage of acidic contents in the LAMP2-deficient neurons. Scale bar: 10 μm.

Figure 4: LAMP2-deficient neurons showed increase levels of cytosolic cathepsin L. (A) Western blot analysis revealed the elevated level of active cathepsin L in the LAMP2-deficient iPSCs-derived cortical neurons under non-stressed condition. (**B**) Western blot analysis showed that oxidative stress increased the abundance of active cathepsin L in the cytosols. N = 3; *: $P<0.05$

Figure 5 Cathepsin L-specific inhibitor ameliorated the oxidative stress-induced apoptosis in LAMP2-deficient iPSCs-derived cortical neurons. (**A**) The cells of interest were supplemented with different concentrations of cathepsin L-specific inhibitor and subjected to mild oxidative stress for 24 hr, the relative cell viabilities were evaluated using MTT Assay. The values of the groups without oxidative stress treatment were assigned as 100% viable. n = 4, ***: $P<0.001$ comparing to the groups treated with 10 μM H_2O_2 in the absence of cathepsin L-inhibitor. (**B**) Cathepsin L inhibitor significantly reduced the mild oxidative stress-induced apoptosis in LAMP2-deficient iPSCs-derived cortical neurons. n = 4, ***: $P<0.01$. (**C**) LAMP2-deficient iPSCs-derived cortical neurons treated 10 μM H_2O_2 in the presence or absence of cathepsin L inhibitor, and the percentage of caspase-3/7 active cells were evaluated with the CellEvent Caspase-3/7 Green Detection Reagent. Scale bar: 40 μm. n = 1000 cells from 3-7 fields for each group, ***: $P<0.001$

Highlights

- We generated iPSCs from patients with *LAMP2*-c.183_184insA mutation
- We differentiated the patient specific iPSCs into LAMP2-deficient cortical neurons.
- The LAMP2-deficient neurons are more susceptible to oxidative stress induced cell death.
- Cathepsin L inhibitor ameliorated the oxidative stress induced cell death observed in the LAMP2-deficient neurons.

Figure 1

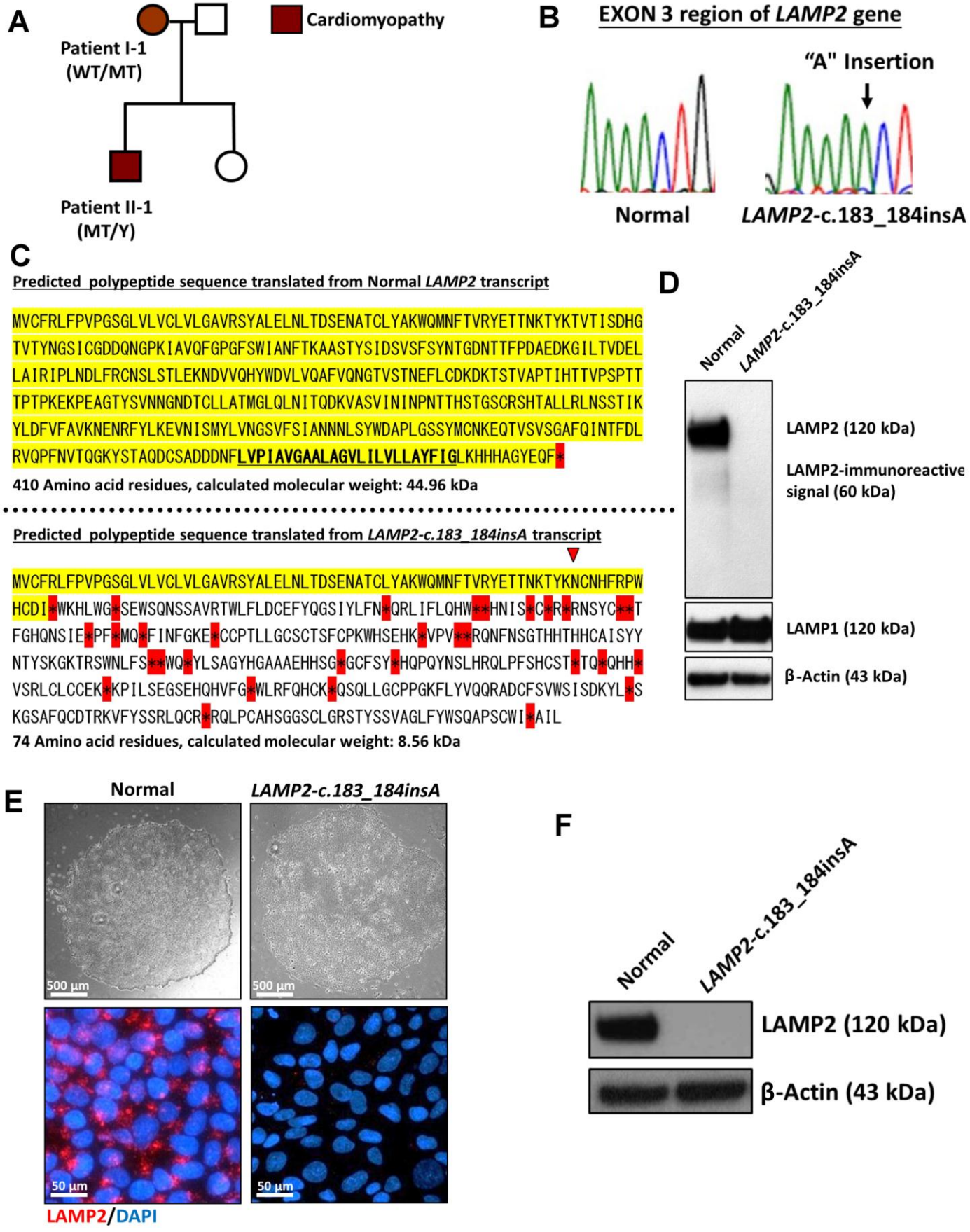

Figure 2

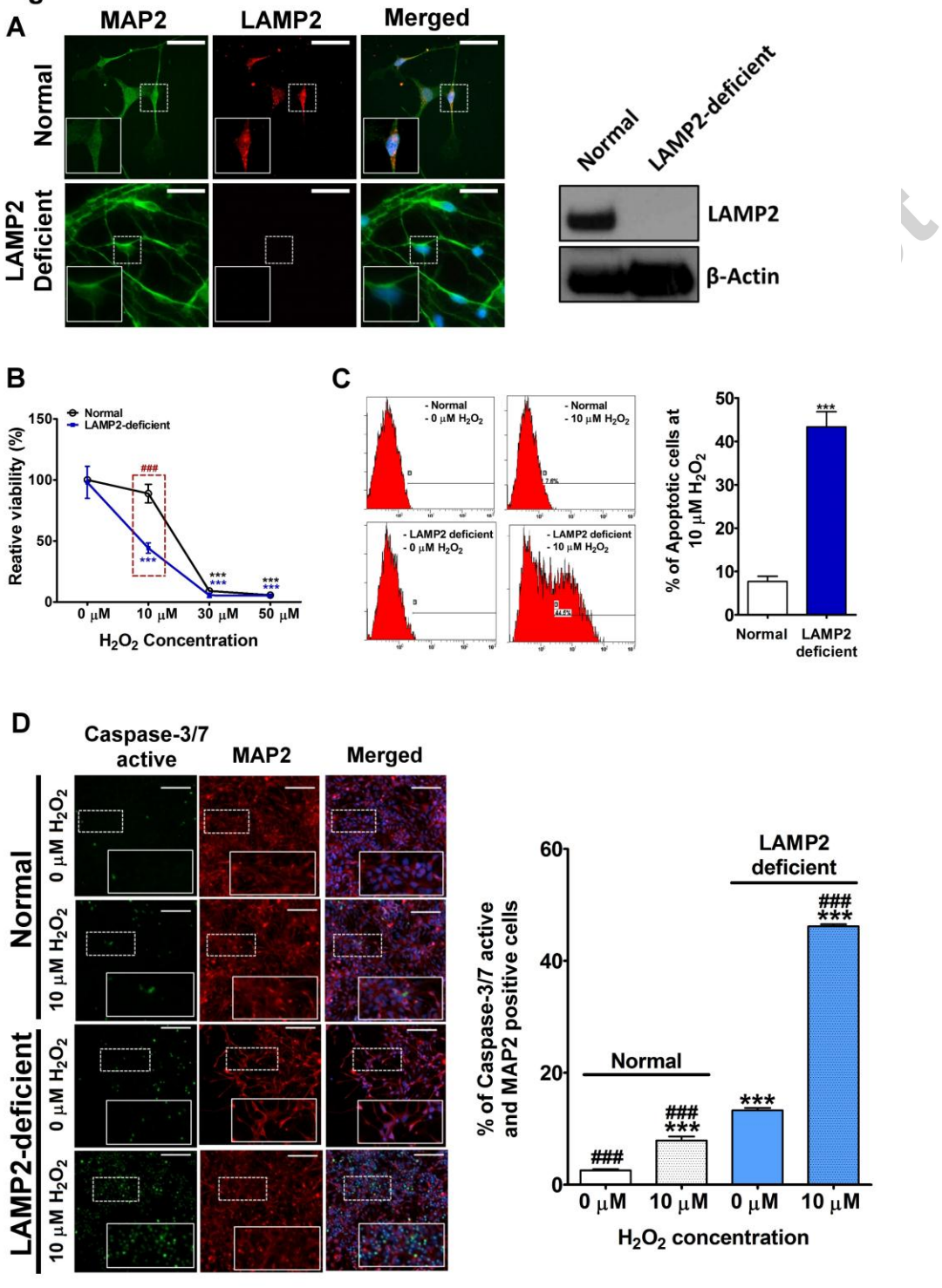
A
MAP2
LAMP2
Merged
Normal
LAMP2 Deficient
Normal
LAMP2-deficient
LAMP2
β-Actin
B
Normal
LAMP2-deficient
Reative viability (%)
150
100
50
0
###
***
0 μM
10 μM
30 μM
50 μM
H2O2 Concentration
C
- Normal
- 0 μM H2O2
- Normal
- 10 μM H2O2
- LAMP2 deficient
- 0 μM H2O2
- LAMP2 deficient
- 10 μM H2O2
% of Apoptotic cells at 10 μM H2O2
50
40
30
20
10
0
***
Normal
LAMP2 deficient
D
Caspase-3/7 active
MAP2
Merged
Normal
0 μM H2O2
10 μM H2O2
LAMP2-deficient
0 μM H2O2
10 μM H2O2
% of Caspase-3/7 active and MAP2 positive cells
60
40
20
0
Normal
LAMP2 deficient
###
***
0 μM
10 μM
0 μM
10 μM
H2O2 concentration

Figure 3

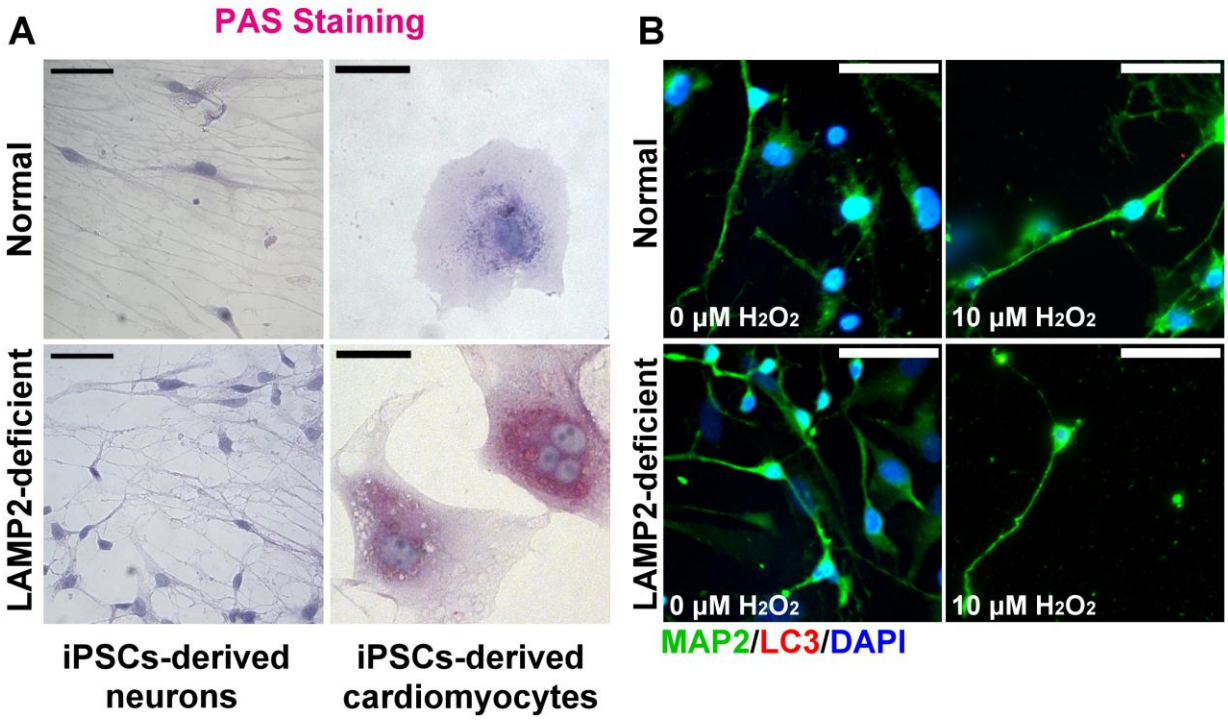
A
PAS Staining
Normal
LAMP2-deficient
iPSCs-derived neurons
iPSCs-derived cardiomyocytes
B
Normal
LAMP2-deficient
0 μM H2O2
10 μM H2O2
0 μM H2O2
10 μM H2O2
MAP2/LC3/DAPI
C
Normal
LAMP2-deficient

Figure 4

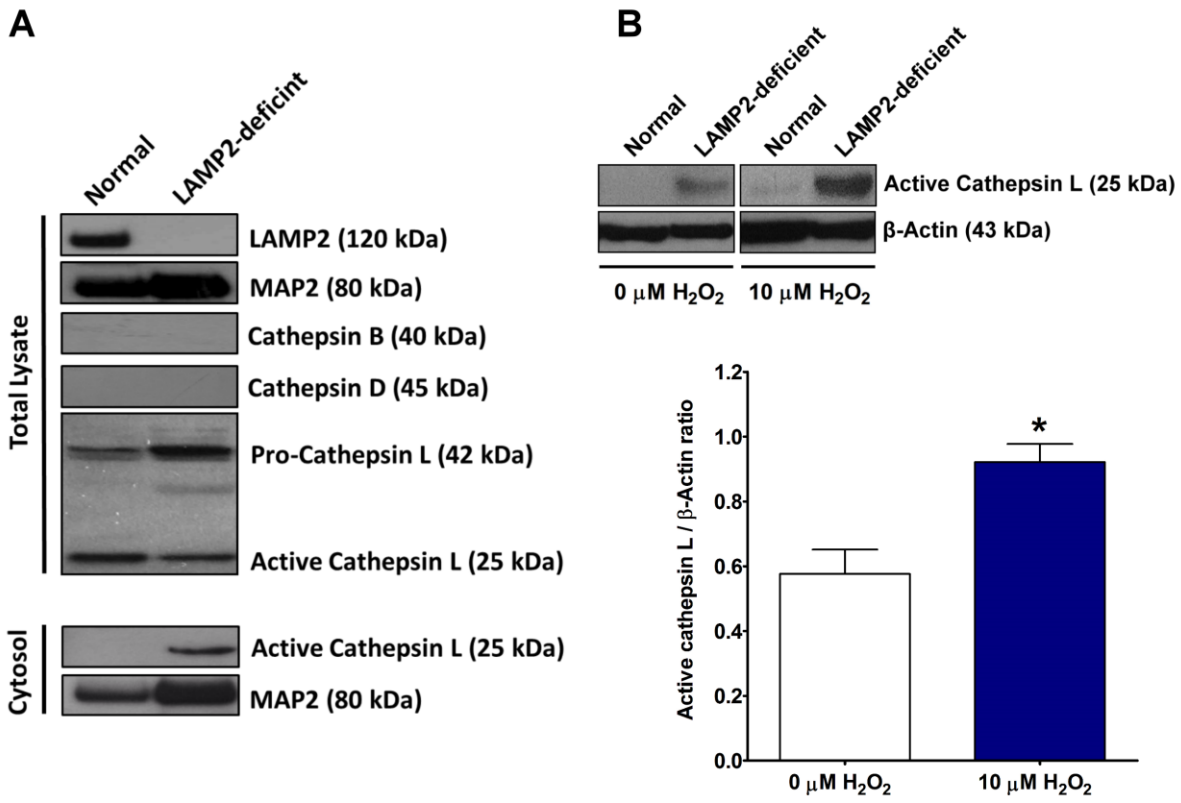
A
Normal
LAMP2-deficint
Total Lysate
LAMP2 (120 kDa)
MAP2 (80 kDa)
Cathepsin B (40 kDa)
Cathepsin D (45 kDa)
Pro-Cathepsin L (42 kDa)
Active Cathepsin L (25 kDa)
Cytosol
Active Cathepsin L (25 kDa)
MAP2 (80 kDa)
B
Normal
LAMP2-deficient
Normal
LAMP2-deficient
Active Cathepsin L (25 kDa)
β-Actin (43 kDa)
0 μM H2O2
10 μM H2O2
Active cathepsin L / β-Actin ratio
1.2
1.0
0.8
0.6
0.4
0.2
0.0
*
0 μM H2O2
10 μM H2O2

Figure 5

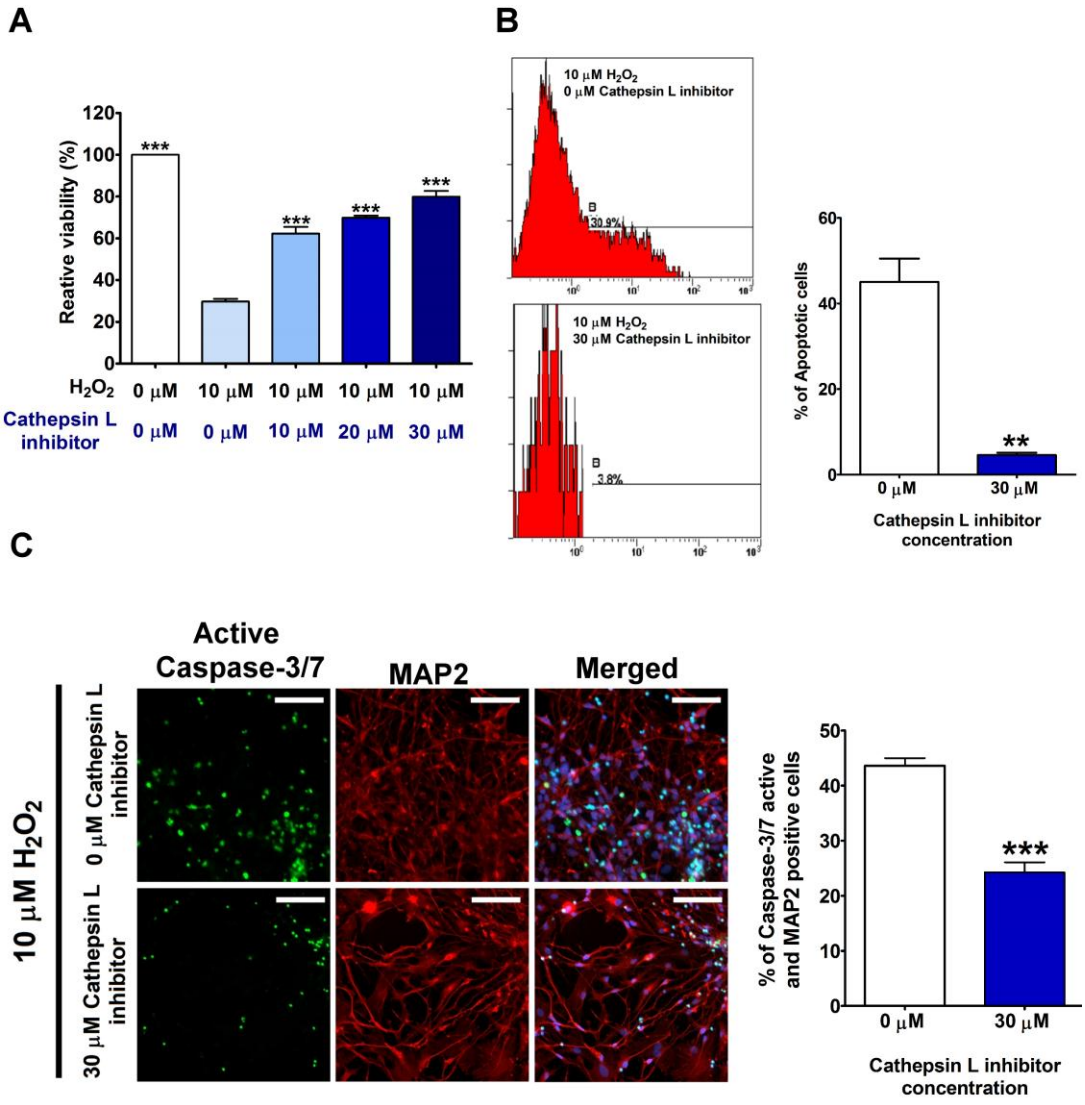
A
B
C
Reative viability (%)
120
100
80
60
40
20
0
***
H_2O_2 0 μM 10 μM 10 μM 10 μM 10 μM
Cathepsin L inhibitor 0 μM 0 μM 10 μM 20 μM 30 μM
10 μM H_2O_2
0 μM Cathepsin L inhibitor
B
30.9%
10 μM H_2O_2
30 μM Cathepsin L inhibitor
B
3.8%
% of Apoptotic cells
60
40
20
0
**
0 μM
30 μM
Cathepsin L inhibitor concentration
Active Caspase-3/7
MAP2
Merged
10 μM H_2O_2
0 μM Cathepsin L inhibitor
30 μM Cathepsin L inhibitor
% of Caspase-3/7 active and MAP2 positive cells
50
40
30
20
10
0
***
0 μM
30 μM
Cathepsin L inhibitor concentration